Supplemental Materials: Methylphenidate stabilizes dynamic brain network organization during tasks probing attention and reward processing in stimulant-naïve children with ADHD.

Tehila Nugiel*[1], Nicholas D. Fogleman[2,3], Monica G. Lyons[3], Margaret A. Sheridan[3], Jessica R. Cohen[3]

[1]Department of Psychology, Florida State University, Tallahassee Florida

[2]Department of Psychiatry, University of North Carolina at Chapel Hill, Chapel Hill, North Carolina

[3]Department of Psychology and Neuroscience, University of North Carolina at Chapel Hill, Chapel Hill, North Carolina

*Corresponding author
Tehila Nugiel
Department of Psychology
Florida State University
1107 W Call St.
Tallahassee, FL 32304
Email: tnugiel@fsu.edu

Supplemental Table 1. The number of subjects contributing each number of runs to standard go/no-go analyses after runs were excluded based on quality control criteria.

Number of subjects	Number of standard go/no-go runs MPH	Number of standard go/no-go runs placebo
1	1	1
4	1	2
6	2	1
17	2	2

Supplemental Table 2. The number of subjects contributing each number of runs to rewarded go/no-go analyses after runs were excluded based on quality control criteria.

Number of subjects	Number of rewarded go/no-go runs MPH	Number of rewarded go/no-go runs placebo
1	1	4
1	2	2
1	2	3
1	3	1
2	3	3
3	3	4
2	4	1
1	4	2
4	4	3
13	4	4

fMRI processing details:

Results included in this manuscript come from preprocessing performed using *fMRIPrep* 21.0.2 (Esteban, Markiewicz, et al., 2018; Esteban, Blair, et al., 2018; RRID:SCR_016216), which is based on *Nipype* 1.6.1 (K. Gorgolewski et al., 2011; K. J. Gorgolewski et al., 2018; RRID:SCR_002502).

Anatomical data preprocessing

A total of 1 T1-weighted (T1w) images were found within the input BIDS dataset.The T1-weighted (T1w) image was corrected for intensity non-uniformity (INU) with N4BiasFieldCorrection (Tustison et al., 2010), distributed with ANTs 2.3.3 (Avants et al., 2008, RRID:SCR_004757), and used as T1w-reference throughout the workflow. The T1w-reference was then skull-stripped with a *Nipype* implementation of the antsBrainExtraction.sh workflow (from ANTs), using OASIS30ANTs as target template. Brain tissue segmentation of cerebrospinal fluid (CSF), white-matter (WM) and gray-matter (GM) was performed on the brain-extracted T1w using fast (FSL 6.0.5.1:57b01774, RRID:SCR_002823, Zhang, Brady, and Smith, 2001). Brain surfaces were reconstructed using recon-all (FreeSurfer 6.0.1, RRID:SCR_001847, Dale, Fischl, and Sereno, 1999), and the brain mask estimated previously was refined with a custom variation of the method to reconcile ANTs-derived and FreeSurfer-derived segmentations of the cortical gray-matter of Mindboggle (RRID:SCR_002438, Klein et al., 2017). Volume-based spatial normalization to two standard spaces (MNI152NLin2009cAsym, MNI152NLin6Asym) was performed through nonlinear registration with antsRegistration (ANTs 2.3.3), using brain-extracted versions of both T1w reference and the T1w template. The following templates were selected for spatial normalization: *ICBM 152 Nonlinear Asymmetrical template version 2009c* [Fonov et al., 2009, RRID:SCR_008796; TemplateFlow ID: MNI152NLin2009cAsym], *FSL's MNI ICBM 152 non-linear 6th Generation Asymmetric Average Brain Stereotaxic Registration Model* [Evans et al., 2012, RRID:SCR_002823; TemplateFlow ID: MNI152NLin6Asym].

Functional data preprocessing

For each of the 12 BOLD runs found per subject (across all tasks and sessions), the following preprocessing was performed. First, a reference volume and its skull-stripped version were generated using a custom methodology of *fMRIPrep*. Head-motion parameters with respect to the BOLD reference (transformation matrices, and six corresponding rotation and translation parameters) were estimated before any spatiotemporal filtering using mcflirt (FSL 6.0.5.1:57b01774, Jenkinson et al., 2002). BOLD runs were slice-time corrected to 0.964s (0.5 of slice acquisition range 0s-1.93s) using 3dTshift from AFNI (Cox and Hyde, 1997, RRID:SCR_005927). The BOLD time-series (including slice-timing correction) were resampled onto their original, native space by applying the transforms to correct for head-motion. These resampled BOLD time-series will be referred to as *preprocessed BOLD in original space*, or just *preprocessed BOLD*. The BOLD reference was then co-registered to the T1w reference using bbregister (FreeSurfer), which implements boundary-based registration (Greve and Fischl, 2009). Co-registration was configured with six degrees of freedom. Several confounding time-series were calculated based on the *preprocessed BOLD*: framewise displacement (FD), and

three region-wise global signals. FD was computed using two formulations following Power (absolute sum of relative motions, Power et al.,2014) and Jenkinson (relative root mean square displacement between affines, Jenkinson et al., 2002). FD was calculated for each functional run, using implementation in *Nipype* (following the definitions by Power et al., 2014). The three global signals were extracted within the CSF, the WM, and the whole-brain masks. The head-motion estimates calculated in the correction step were also placed within the corresponding confounds file. The confound time series derived from head motion estimates and global signals were expanded with the inclusion of temporal derivatives and quadratic terms for each (Satterthwaite et al., 2013). The BOLD time-series were resampled into standard space, generating a *preprocessed BOLD run in MNI152NLin2009cAsym space*. First, a reference volume and its skull-stripped version were generated using a custom methodology of *fMRIPrep*. Automatic removal of motion artifacts using independent component analysis (ICA-AROMA, Pruim et al., 2015) was performed on the *preprocessed BOLD on MNI space* time-series after removal of non-steady state volumes and spatial smoothing with an isotropic, Gaussian kernel of 6mm FWHM (full-width half-maximum). Additionally, the “aggressive” noise-regressors were collected and placed in the corresponding confounds file. All resamplings can be performed with *a single interpolation step* by composing all the pertinent transformations (i.e. head-motion transform matrices, and co-registrations to anatomical and output spaces). Gridded (volumetric) resamplings were performed using antsApplyTransforms (ANTs), configured with Lanczos interpolation to minimize the smoothing effects of other kernels (Lanczos, 1964). Non-gridded (surface) resamplings were performed using mri_vol2surf (FreeSurfer).

Many internal operations of *fMRIPrep* use *Nilearn* 0.8.1 (Abraham et al., 2014, RRID:SCR_001362), mostly within the functional processing workflow. For more details of the pipeline, see the section corresponding to workflows in *fMRIPrep*’s documentation.

Analyses with stimulus event regression:

To test for the effects of stimulus events on time-varying connectivity, we ran supplemental analyses regressing out stimulus events in addition to the standard nuisance regressors (AROMA ICA, cerebrospinal fluid, white matter, and global signal) from the timeseries before the dynamic conditional correlation (DCC) step. To do so, we included a separate regressor for each stimulus type (correct go, incorrect go, omissions, commissions, correct no-go, premature responses < 200 ms, and slow correct go responses > 650 ms) and their temporal derivatives. The regressors were convolved using a double-gamma hemodynamic response function (HRF) and filtered with a high pass filter (0.08 mHz). These regressors were then added to the regression matrix along with the other nuisance regressors described in the *Methods* sections of the main text. All confound signals were then regressed from the timeseries in one step.

Whole brain flexibility differences between MPH and placebo with stimulus event regression

Similar to the effects reported in the *Results* section of the main text, whole brain flexibility was lower on MPH than on placebo, though the effects were smaller when stimulus events were included as nuisance regressors. During the standard go/no-go task, whole brain flexibility was lower on MPH than on placebo, however this effect did not reach significance (b = 0.003, uncorrected-p = 0.12, corrected-p = 0.12; mean placebo = .044(0.01), mean MPH = .041(0.01), Supplemental Figure 1a). During the rewarded go/no-go task, whole brain flexibility was significantly lower on MPH than on placebo (b = 0.003, uncorrected-p = 0.01, corrected-p = 0.03; mean placebo = .041(0.01), mean MPH = .038(0.009), Supplemental Figure 1b). Confidence intervals on standardized effects were almost entirely overlapping across these supplemental analyses and those reported in the main text (standard go/no-go: stimulus event regressed = -0.08-0.67, non-stimulus event regressed = 0.09-0.68; rewarded go/no-go: stimulus event regressed = 0.06-0.57, non-stimulus event regressed = 0.18-0.64). Importantly, neither result changed significantly when testing for an interaction of with/without task regression (all uncorrected p-values on interaction terms > 0.25). The consistency in direction and lack of significant difference between the effects with and without stimulus event regression suggests that the effects reported in the main text are not due to spurious effects on connectivity of stimulus events. The reduced size of effects observed here are likely due to a combination of reduced degrees of freedom and the removal of cognitively relevant task-related signals.

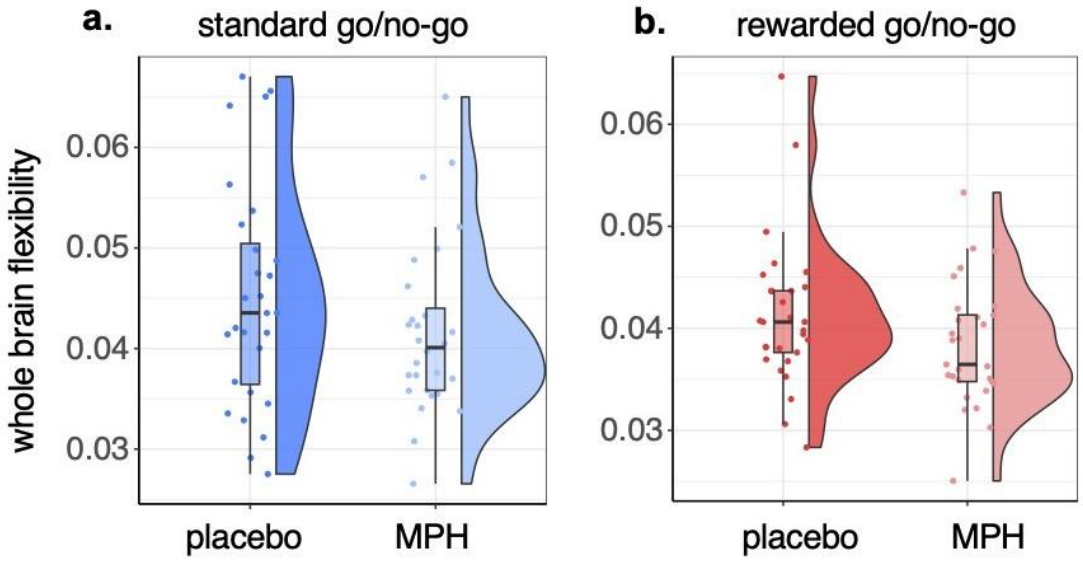

Supplemental Figure 1. Whole brain flexibility estimated after stimulus events were regressed out of the timeseries decreased on MPH a) during the standard go/no-go task (*b*= 0.003, uncorrected-*p* = 0.12, corrected-*p* = 0.12) and b) during the rewarded go/no-go task (*b*= 0.003, uncorrected-*p* = 0.01, corrected-*p* = 0.03). Error bars on boxplots represent the 25th and 75th quartile.

Changes in task performance related to changes in whole brain flexibility with stimulus event regression

We next tested the relationship between the change in whole brain flexibility and changes in both tau and d' when stimulus events were regressed out of the timeseries. As with the whole brain changes in flexibility reported above, effects were similar to those reported in the *Results* section of the main text, though the effects were weakened and none of the correlations below were statistically significant after multiple comparison correction. During the standard go/no-go task, change in whole brain flexibility was positively correlated with change in tau ($r(26) = 0.39$, uncorrected-p = .04, corrected-p = .16; Supplemental Figure 2a). During the rewarded go/no-go task, change in whole brain flexibility was similarly positively correlated with change in tau: ($r(27) = 0.21$, uncorrected-p = .26, corrected-p = .35; Supplemental Figure 2b). During the rewarded go/no-go task, change in whole brain flexibility was negatively correlated with change in d' ($r(27) = -0.32$, uncorrected-p = .09, corrected-p = .35, Supplemental Figure 2c). Finally, during the standard go/no-go task, change in whole brain flexibility remained negatively and not significantly correlated with d' ($r(26) = -0.14$, uncorrected-p = 0.48, corrected p =0.86).Similar to the whole brain changes in flexibility reported above, none of these results changed significantly when conducting direct comparisons between those reported in the *Main Text* and here (all z-values ≤ 0.88, all p-values ≥ 0.37, uncorrected), once again indicating that the effects reported in the main text are not due to spurious effects on connectivity of stimulus events. As stated

above, the reduced size of effects are likely due to reduced degrees of freedom and the removal of cognitively relevant task-related signals.

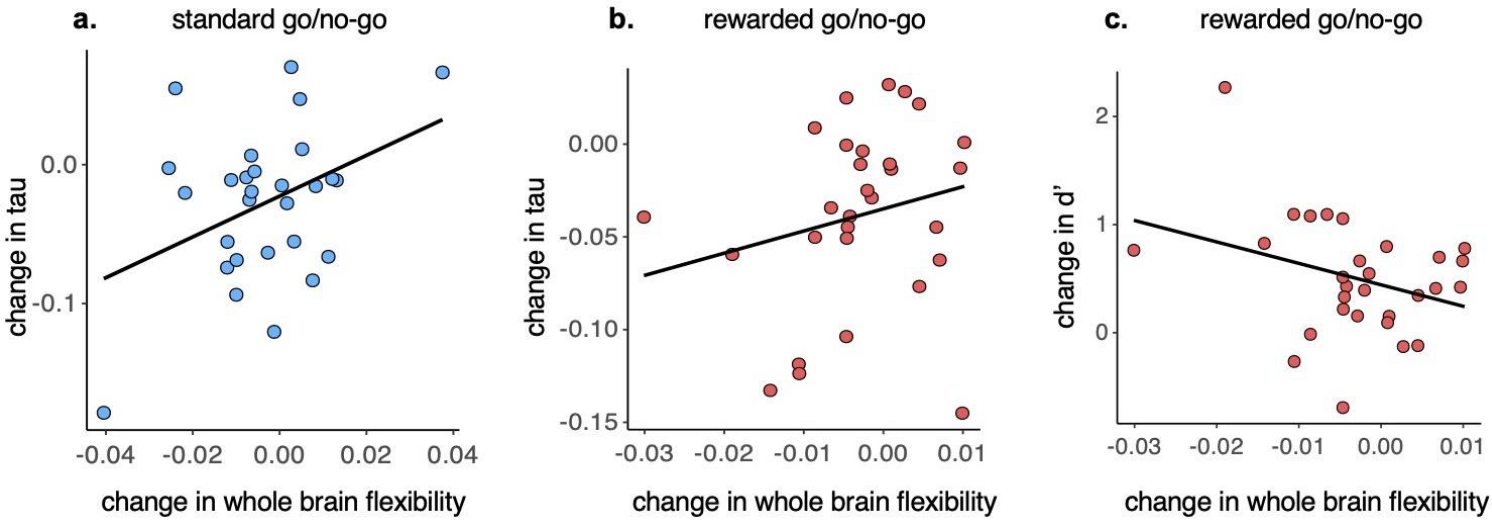

Supplemental Figure 2. Relationships between change in whole brain flexibility and change in behavior estimated after with stimulus events were regressed out of the timeseries were not significant but were in the same direction as findings reported in the *Main Text*. Change in whole brain flexibility on MPH was related to a) change in tau during the standard go/no-go task ($r(26) = 0.39$, uncorrected-$p = .04$, corrected-$p = .16$), b) change in tau during the rewarded go/no-go task ($r(27) = 0.21$, uncorrected-$p = .26$, corrected-$p = .35$), and c) change in d' during the rewarded go/no-go task ($r(27) = -0.32$, uncorrected-$p = .09$, corrected-$p = .35$). Change for all measures was calculated as MPH - placebo.

Testing for the effects of multilayer modularity parameters

The multilayer modularity algorithm has two free parameters: γ, which modulates within-layer connections, and ω, which modulates between-layer connections. As levels of γ increase the number of communities increases and communities generally become smaller. As levels of ω increase there are fewer changes in community assignment between layers. In order to match the number of brain networks in our chosen atlas (12; Seitzman et al., 2020), in primary analyses we specified the modularity parameter γ to be 1.5, which led to an average of 10.96 communities per layer. We specified the modularity parameter ω to not bias intralayer changes in communities (Telesford et al. 2016).

To test for the sensitivity of effects across varying values of γ and ω, we ran a supplemental set of analyses in which we tested the effect of MPH on whole brain flexibility over a range of combinations of γ and ω tested at increments of .25 from 1-2. These effects are reported in Supplemental Table 3. Generally, effects were in a consistent direction, particularly for the rewarded go/no-go task. The effects reported in the main text typically did not hold at combinations of higher values of γ and ω. This is to be expected, as at higher values e communities would be small and fragmented and there would be few between-layer changes in community assignment. Both of these features would constrain time-varying functional connectivity.

Supplemental Table 3. Standardized betas for the main effect of drug condition on whole brain flexibility tested across multilayer parameters.

standard go/no-go	**γ 1**	**γ 1.25**	**γ 1.5**	**γ 1.75**	**γ 2**
ω 1	0.2	0.17	*0.38	0.30	*0.37
ω 1.25	0.25	0.12	*0.43	0.14	0.14
ω 1.5	0.25	0.19	0.08	0.01	0.07
ω 1.75	*0.28	0.19	-0.03	0.02	0.21
ω 2	*0.41	-0.03	-0.15	0.08	0.29
rewarded go/no-go	**γ 1**	**γ 1.25**	**γ 1.5**	**γ 1.75**	**γ 2**
ω 1	0.19	*0.34	*0.41	0.23	0.24
ω 1.25	0.19	*0.45	*0.38	0.14	0.10
ω 1.5	0.22	*0.34	*0.25	0.21	0.07
ω 1.75	*0.25	*0.25	0.04	0.06	0.10
ω 2	*0.25	0.14	-0.01	0.14	0.03

Main effects were computed at increments of .25 from 1-2 for γ and ω.*denotes a significant uncorrected *p*-value.

We additionally tested the relationships between change in whole brain flexibility and change in tau (Supplemental Table 4), as well as between change in whole brain flexibility and change in d' (Supplemental Table 5) across the same range of combinations of γ and Ω (increments of .25 spanning 1-2). The relationships between change in whole brain flexibility and change in tau were more consistent during the standard go/no-go than the rewarded go/no-go task. Relationships between change in whole brain flexibility and change in d' during the standard go/no-go were mostly consistently null, as they were in the main text. The relationship between change in whole brain flexibility and change in d' during the rewarded go/no-go task were consistent and significant across many combination of γ and Ω.

Supplemental Table 4. Correlation values for the relationship between change in whole brain flexibility and change in tau tested across multilayer parameters.

standard go/no-go tau	**γ 1**	**γ 1.25**	**γ 1.5**	**γ 1.75**	**γ 2**
Ω 1	0.29	-0.03	*0.43	*0.42	0.36
Ω 1.25	0.16	0.04	*0.46	*0.43	0.18
Ω 1.5	-0.04	*0.38	0.3	0.32	0.14
Ω 1.75	0.04	.07	0.07	0.10	0.21
Ω 2	0.12	.04	-0.03	0.06	0.22
rewarded go/no-go tau	**γ 1**	**γ 1.25**	**γ 1.5**	**γ 1.75**	**γ 2**
Ω 1	0.04	0.16	*0.43	0.16	0.02
Ω 1.25	-0.03	0.22	0.2	-0.07	-0.08
Ω 1.5	0.07	0.07	0.10	0.13	0.04
Ω 1.75	0.11	0.05	-0.10	0.04	-0.09
Ω 2	0.10	0.11	0.02	-0.06	-0.02

Pearson correlations were computed at increments of .25 from 1-2 for γ and Ω. *denotes a significant uncorrected p-value on the effect.

Supplemental Table 5. Correlation values for the relationship between change in whole brain flexibility and change in d' tested across multilayer parameters.

standard go/no-go d'	**γ 1**	**γ 1.25**	**γ 1.5**	**γ 1.75**	**γ 2**
ω 1	-0.25	-0.04	-0.03	-0.26	-0.07
ω 1.25	*-0.44	-0.06	-0.09	-0.08	-0.07
ω 1.5	-0.30	-0.10	0.04	-0.01	-0.1
ω 1.75	-0.24	0.07	0.06	0.07	-0.01
ω 2	-0.22	-0.13	0.16	0.05	-0.09
rewarded go/no-go d'	**γ 1**	**γ 1.25**	**γ 1.5**	**γ 1.75**	**γ 2**
ω 1	-0.36	*-0.73	*-0.47	*-0.48	-0.36
ω 1.25	-0.24	*-0.74	*-0.45	*-0.41	*-0.41
ω 1.5	-0.26	*-0.69	*-0.61	*-0.42	-0.18
ω 1.75	-0.36	*-0.60	-0.31	-0.36	-0.28
ω 2	*-0.41	*0.49	-0.27	-0.28	-0.23

Pearson correlations were computed at increments of .25 from 1-2 for γ and ω. *denotes a significant uncorrected p-value on the effect.

Taken together, these sensitivity analyses suggest that when multilayer parameters recapitulate canonical large-scale brain networks most of our reported effects are consistent. However, when γ is high, which would lead to many small communities, or when ω is high, which would constrain changes in communities across time, the reported effects are diminished. These sensitivity analyses indicate the importance of selecting parameters to recapitulate canonical large-scale functional brain networks (i.e., when the number of communities per layer are aligned with the chosen brain atlas).

Supplemental Table 6. Regressions predicting change in task performance from change in whole brain flexibility, with change in head motion, sex, and age, as covariates.

change in tau standard go/no-go	**predictor**	***b***	***B***	***SE***	***t***	***uncorrected-p***
	Change in whole brain flexibility*	3.17	0.56	1.02	3.12	0.005
	Change in FD	-0.17	-0.35	0.08	-2.16	0.041
	Sex	-0.01	-0.15	0.02	-0.46	0.649
	Age	0.02	0.36	0.01	2.01	0.056
change in tau rewarded go/no-go						
	Change in whole brain flexibility*	2.80	0.46	1.13	2.49	0.020
	Change in FD	0.05	0.09	0.11	0.51	0.617
	Sex	0.02	0.33	0.02	0.92	0.368
	Age	0.00	-0.10	0.01	-0.52	0.611
change in d' standard go/no-go						
	Change in whole brain flexibility	6.80	0.11	12.90	0.53	0.603
	Change in FD	2.12	0.39	0.99	2.14	0.044
	Sex	0.30	0.49	0.23	1.31	0.202
	Age	0.10	0.19	0.11	0.93	0.362
change in d' rewarded go/no-go						
	Change in whole brain flexibility*	-33.04	-0.45	12.77	-2.59	0.016
	Change in FD	1.89	0.27	1.23	1.54	0.138
	Sex	-0.13	-0.21	0.20	-0.62	0.540
	Age	0.01	0.02	0.09	0.14	0.889

Change for all measures was calculated as MPH - placebo except for head motion, which was calculated as placebo - MPH. FD = framewise displacement *denotes $p < .05$ after FDR correction for multiple comparisons. SE = standard error.

References

Abraham, Alexandre, Fabian Pedregosa, Michael Eickenberg, Philippe Gervais, Andreas Mueller, Jean Kossaifi, Alexandre Gramfort, Bertrand Thirion, and Gael Varoquaux. 2014. “Machine Learning for Neuroimaging with Scikit-Learn.” *Frontiers in Neuroinformatics* 8. https://doi.org/10.3389/fninf.2014.00014.

Avants, B. B., C. L. Epstein, M. Grossman, and J. C. Gee. 2008. “Symmetric Diffeomorphic Image Registration with Cross-Correlation: Evaluating Automated Labeling of Elderly and Neurodegenerative Brain.” *Medical Image Analysis* 12 (1):

Cox, Robert W., and James S. Hyde. 1997. “Software Tools for Analysis and Visualization of fMRI Data.” *NMR in Biomedicine* 10 (4-5): 171–78. https://doi.org/10.1002/(SICI)1099-1492(199706/08)10:4/5<171::AID-NBM453>3.0.CO;2-L.

Dale, Anders M., Bruce Fischl, and Martin I. Sereno. 1999. “Cortical Surface-Based Analysis: I. Segmentation and Surface Reconstruction.” *NeuroImage* 9 (2): 179–94. https://doi.org/10.1006/nimg.1998.0395.

Esteban, Oscar, Ross Blair, Christopher J. Markiewicz, Shoshana L. Berleant, Craig Moodie, Feilong Ma, Ayse Ilkay Isik, et al. 2018. “fMRIPrep.” *Software*. https://doi.org/10.5281/zenodo.852659.

Esteban, Oscar, Christopher Markiewicz, Ross W Blair, Craig Moodie, Ayse Ilkay Isik, Asier Erramuzpe Aliaga, James Kent, et al. 2018. “fMRIPrep: A Robust Preprocessing Pipeline for Functional MRI.” *Nature Methods*. https://doi.org/10.1038/s41592-018-0235-4.

Evans, AC, AL Janke, DL Collins, and S Baillet. 2012. “Brain Templates and Atlases.” *NeuroImage* 62 (2): 911–22. https://doi.org/10.1016/j.neuroimage.2012.01.024.

Fonov, VS, AC Evans, RC McKinstry, CR Almli, and DL Collins. 2009. “Unbiased Nonlinear Average Age-Appropriate Brain Templates from Birth to Adulthood.” *NeuroImage* 47, Supplement 1: S102. https://doi.org/10.1016/S1053-8119(09)70884-5.

Gorgolewski, K., C. D. Burns, C. Madison, D. Clark, Y. O. Halchenko, M. L. Waskom, and S. Ghosh. 2011. “Nipype: A Flexible, Lightweight and Extensible Neuroimaging Data Processing Framework in Python.” *Frontiers in Neuroinformatics* 5: 13. https://doi.org/10.3389/fninf.2011.00013.

Gorgolewski, Krzysztof J., Oscar Esteban, Christopher J. Markiewicz, Erik Ziegler, David Gage Ellis, Michael Philipp Notter, Dorota Jarecka, et al. 2018. “Nipype.” *Software*. https://doi.org/10.5281/zenodo.596855.

Greve, Douglas N, and Bruce Fischl. 2009. “Accurate and Robust Brain Image Alignment Using Boundary-Based Registration.” *NeuroImage* 48 (1): 63–72. https://doi.org/10.1016/j.neuroimage.2009.06.060.

Jenkinson, Mark, Peter Bannister, Michael Brady, and Stephen Smith. 2002. “Improved Optimization for the Robust and Accurate Linear Registration and Motion Correction of Brain Images.” *NeuroImage* 17 (2): 825–41. https://doi.org/10.1006/nimg.2002.1132.

Klein, Arno, Satrajit S. Ghosh, Forrest S. Bao, Joachim Giard, Yrjö Häme, Eliezer Stavsky, Noah Lee, et al. 2017. “Mindboggling Morphometry of Human Brains.” *PLOS Computational Biology* 13 (2): e1005350. https://doi.org/10.1371/journal.pcbi.1005350.

Lanczos, C. 1964. “Evaluation of Noisy Data.” *Journal of the Society for Industrial and Applied Mathematics Series B Numerical Analysis* 1 (1): 76–85. https://doi.org/10.1137/0701007.

Power, Jonathan D., Anish Mitra, Timothy O. Laumann, Abraham Z. Snyder, Bradley L. Schlaggar, and Steven E. Petersen. 2014. “Methods to Detect, Characterize, and Remove Motion Artifact in Resting State fMRI.” *NeuroImage* 84 (Supplement C): 320–41. https://doi.org/10.1016/j.neuroimage.2013.08.048.

Pruim, Raimon H. R., Maarten Mennes, Daan van Rooij, Alberto Llera, Jan K. Buitelaar, and Christian F. Beckmann. 2015. “ICA-AROMA: A Robust ICA-Based Strategy for Removing Motion Artifacts from fMRI Data.” *NeuroImage* 112 (Supplement C): 267–77. https://doi.org/10.1016/j.neuroimage.2015.02.064.

Satterthwaite, Theodore D., Mark A. Elliott, Raphael T. Gerraty, Kosha Ruparel, James Loughead, Monica E. Calkins, Simon B. Eickhoff, et al. 2013. “An improved framework for confound regression and filtering for control of motion artifact in the preprocessing of resting-state functional connectivity data.” *NeuroImage* 64 (1): 240–56. https://doi.org/10.1016/j.neuroimage.2012.08.052.

Seitzman, B. A., Gratton, C., Marek, S., Raut, R. V., Dosenbach, N. U., Schlaggar, B. L., ... & Greene, D. J. (2020). A set of functionally-defined brain regions with improved representation of the subcortex and cerebellum. *Neuroimage*, *206*, 116290 https://doi.org/10.1016/j.neuroimage.2019.116290.

Telesford, Q. K., Lynall, M. E., Vettel, J., Miller, M. B., Grafton, S. T., & Bassett, D. S. (2016). Detection of functional brain network reconfiguration during task-driven cognitive states. *NeuroImage*, *142*, 198-210. https://doi.org/10.1016/j.neuroimage.2016.05.078

Tustison, N. J., B. B. Avants, P. A. Cook, Y. Zheng, A. Egan, P. A. Yushkevich, and J. C. Gee. 2010. “N4itk: Improved N3 Bias Correction.” *IEEE Transactions on Medical Imaging* 29 (6): 1310–20. https://doi.org/10.1109/TMI.2010.2046908.

Zhang, Y., M. Brady, and S. Smith. 2001. “Segmentation of Brain MR Images Through a Hidden Markov Random Field Model and the Expectation-Maximization Algorithm.” *IEEE Transactions on Medical Imaging* 20 (1): 45–57. https://doi.org/10.1109/42.906424.